ISSN 1062-8738, Bulletin of the Russian Academy of Sciences: Physics, 2017, Vol. 81, No. 5, pp. 608–611. © Allerton Press, Inc., 2017.
Original Russian Text © S.V. Stolyar, O.A. Bayukov, V.P. Ladygina, R.S. Iskhakov, R.N. Yaroslavtsev, 2017, published in Izvestiya Rossiiskoi Akademii Nauk, Seriya Fizicheskaya, 2017, Vol. 81, No. 5, pp. 660–663.

Effect of Ultrasonic Treatment on Magnetic Ferrihydrite Nanoparticles in a Suspended State

S. V. Stolyar[a, b], O. A. Bayukov[b], V. P. Ladygina[c], R. S. Iskhakov[b, *], and R. N. Yaroslavtsev[a]

[a] *Siberian Federal University, Krasnoyarsk, 660041 Russia*

[b] *Kirensky Institute of Physics, Siberian Branch, Russian Academy of Sciences, Krasnoyarsk, 660036 Russia*

[c] *International Scientific Center for Studying the Extreme States of an Organism, Siberian Branch, Russian Academy of Sciences, Krasnoyarsk, 660036 Russia*

**e-mail: rauf@iph.krasn.ru*

Abstract—Dried sediments of magnetic ferrihydrite nanoparticles subjected to ultrasonic treatment in the cavitation mode are studied via Mössbauer spectroscopy. Fe ions are reduced to the metal state. In all experiments with detected metal reduction, the investigated suspensions contain organic components.

DOI: 10.3103/S1062873817050227

INTRODUCTION

In this work, we present data from Mössbauer spectroscopy investigations of dried suspensions of magnetic nanoparticles subjected to ultrasonic treatment in a suspended state. In [1, 2], we studied specific features of the structure and magnetic properties of ferrihydrite nanoparticles formed by cultivating *Klebsiella oxytoca* bacteria. The investigated particles were 2–3 nm in size. The compound is antiferromagnetic, but becomes ferrimagnetic in the nanodispersed form due to decompensation of the magnetic moments of Fe^{3+} ions on its surface and in the bulk of particles. These particles can compete with ferro- and ferrimagnetic particles in different applications, including directed drug delivery in organisms [3]. We prepared a stable aqueous sol based on biogenic nanoparticles [4]; nuclear magnetic resonance (NMR) tomographic imaging was employed to investigate the distribution of magnetic nanoparticles in the organisms of laboratory animals using different means of infusion [5].

The stability (absence of conglomeration) of the prepared sol of ferrihydrite nanoparticles was ensured by the natural organic shell of the nanoparticles. The functional groups of organic molecules have characteristic vibrations that are reflected in the corresponding absorption bands of infrared (IR) spectra. Such functional groups can therefore be identified by their absorption bands. Figure 1 shows the IR spectra of biogenic ferrihydrite samples, recorded on a Bruker Vertex 80V vacuum Fourier transform spectrometer. The samples were pressed tablets containing potassium bromide, 13 mm in diameter and around 0.55 mm thick. The ferrihydrite particles were thoroughly ground into powder and mixed with KBr (also thoroughly ground) in a ratio of 1 : 100. The mixture was pressed in vacuum by a hydraulic press at pressures of 10 to 104 N cm^{-2}. The IR Fourier spectra contained the peak at 3255.0–3216.2 cm^{-1} typical of valence OH vibrations (Fig. 1) [6]. The peak at 2929.5–2926.8 cm^{-1} corresponds to the CH vibrations of C, and the peak at 1406.2 cm^{-1} is indicative of the presence of O–C–H, C–O–H, and C–C–H groups. These peaks clearly reveal the presence of glucose. In addition, the band at 1311.1 cm^{-1} indicates polysaccharide C–O bonds. These data show that biogenic ferrihydrite nanoparticles were incorporated into iron-binding exopolysaccharides. In addition, the bands at 636.3 and 1546.6 cm^{-1} confirmed the presence of protein amine I and II.

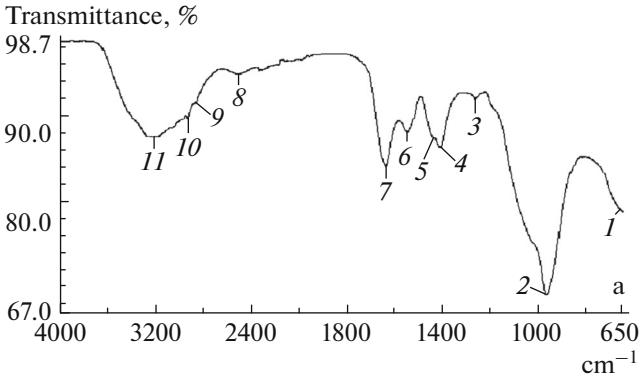

Fig. 1. IR Fourier analysis of ferrihydrite nanoparticles synthesized using *Klebsiella oxytoca* bacteria. Peaks *1* and *2* correspond to the alkenes of =C–H bonds; peak *3*, to carbon and/or hydroxyl CO; peak *4*, to OCH, COH, and CCH groups; peaks *5* and *6*, to protein amides I and II; peak *9*, to the CH vibrations of Cl; peak *10*, to valence OH vibrations.

Since biogenic ferrihydrite nanoparticles have organic shells, we prepared ferrihydrite nanoparticles of the same size (~3 nm) via chemical deposition [7] using iron(III) chloride. The sediment that settled as the potential of hydrogen pH was brought to a neutral value using an alkali solution was collected on a filter, washed, and dried at room temperature. The resulting dry powders were studied via Mössbauer spectroscopy.

The sols of biogenic ferrihydrite nanoparticles and the ferrihydrite nanoparticles prepared by chemical deposition were subjected to ultrasonic treatment in the cavitation mode on a Volna UZTA-0.4/22-OM apparatus (OOO Ultrasonic Technology Center, Biisk). The intensity of ultrasonic treatment was over 10 W cm^{-2} and the frequency was 22 kHz. The treatment time was 4–24 min.

Figure 2 shows the room-temperature Mössbauer spectra of the biogenic ferrihydrite nanoparticles (curve *2*b) and ferrihydrite nanoparticles prepared via chemical deposition (curve *2*a) after ultrasonic treatment in the cavitation mode. Curve *2*b is characterized by a sextet. The results from identifying the spectra (see table) indicate the presence of bcc Fe metal nanoparticles in the sediments of biogenic nanoparticles after cavitation treatment.

The Mössbauer spectra of the ferrihydrite nanoparticles prepared via chemical deposition and subjected to ultrasonic treatment in the cavitation mode remained invariable (curves *2*a and *2*b in Fig. 2). The presence of the bcc Fe phase following cavitation treatment of the ferrihydrite nanoparticles was due to the presence of an organic component. An experiment was performed to confirm this. The chemically deposited and biogenic ferrihydrite nanoparticles were treated with ultrasound in the cavitation mode in a commercial bovine serum albumin (BSA) solution. Figure 2 shows the Mössbauer spectra of the ferrihydrite nanoparticles prepared via chemical deposition and subjected to ultrasonic treatment in the BSA solution (curve *3*a), and of the biogenic ferrihydrite nanoparticles (curve *3*b). Curves *3*a and *3*b are characterized by a sextet. The results from identifying the spectra (see table) indicate the presence of bcc Fe nanoparticles both in the sediments of chemically deposited nanoparticles and in the biogenic nanoparticles after cavitation treatment in the BSA solution.

Mössbauer spectra *2*b, *3*a, and *3*b are thus characterized by a sextet with bcc Fe parameters and the paramagnetic doublet of superparamagnetic ferrihydrite nanoparticles. In the paramagnetic components of spectra *2*a, *3*a, and *3*b, and in spectra *1*a, *1*b, and *2*a, there are three main nonequivalent positions of Fe^{3+} ions with octahedral coordination. These positions can be divided in two groups: positions Fe1 and Fe2 with relatively low local symmetry distortion (QS(Fe1) ~ 0.4–0.5 mm/s and QS(Fe2) ~ 0.7–0.8 mm/s) and positions Fe3 with large distortion (QS(Fe3) ~ 1–1.5).

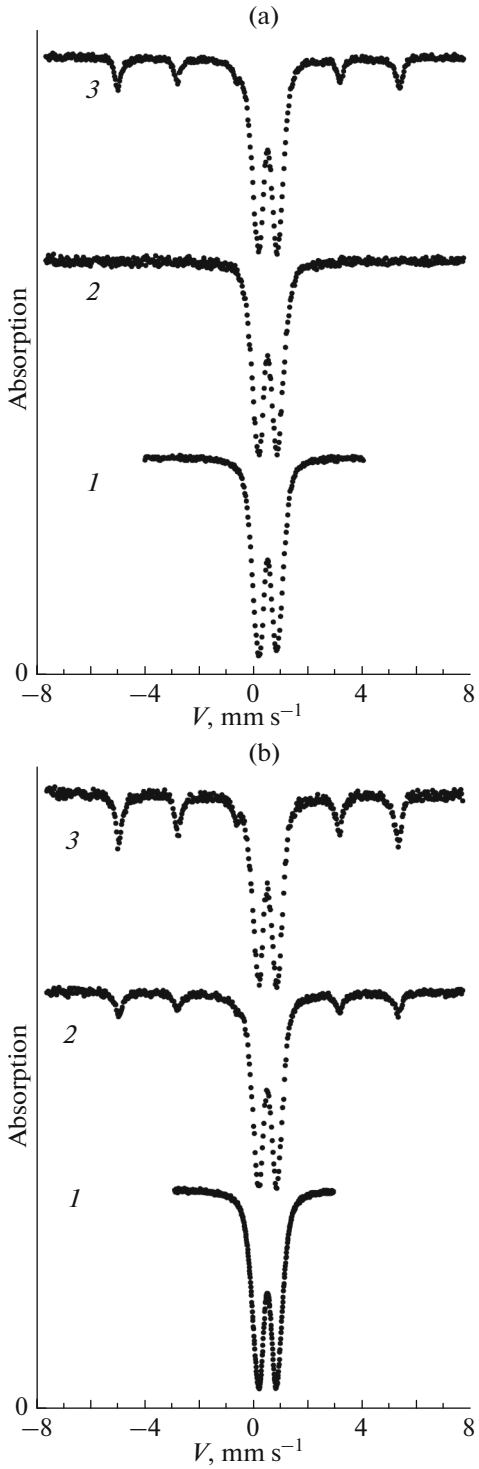

Fig. 2. Mössbauer spectra of (a) chemical and (b) biogenic ferrihydrite. (*1*) Initial particles and particles after ultrasonic treatment in (*2*) water and (*3*) BSA.

The ferrihydrite crystal structure was discussed in [8]. The room-temperature Mössbauer sextets with bcc Fe parameters indicate that the forming ferromagnetic particles were larger than 100 Å [9].

Mössbauer parameters of ferrihydrites. IS is the isomeric shift relative to bcc Fe, QS is quadrupole splitting, W is the width of the absorption line, H is the hyperfine field on an iron core, and A is the fractional population of the position

		IS, mm/s ±0.005	H, kOe ±3	QS, mm/s ±0.02	W, mm/s ±0.02	A, ±0.03	Position
Initial nanoparticles	Chem	0.351		0.51	0.35	0.53	Fe1
		0.355		0.86	0.31	0.37	Fe2
		0.359		1.21	0.26	0.10	Fe3
	Bio	0.349		0.49	0.34	0.43	Fe1
		0.349		0.77	0.32	0.36	Fe2
		0.343		1.10	0.37	0.21	Fe3
Ultrasonic treatment in water	Chem	0.349		0.49	0.33	0.42	Fe1
		0.352		0.79	0.30	0.38	Fe2
		0.355		1.16	0.33	0.20	Fe3
	Bio	0.024	318	0	0.32	0.18	**bcc Fe**
		0.349		0.51	0.35	0.37	Fe1
		0.352		0.80	0.36	0.39	Fe2
		0.348		1.17	0.22	0.06	Fe3
Ultrasonic treatment in BSA	Chem	0.006	332	0	0.25	0.19	**bcc Fe**
		0.350		0.53	0.35	0.35	Fe1
		0.351		0.84	0.36	0.37	Fe2
		0.357		1.22	0.30	0.10	Fe3
	Bio	0.019	318	0	0.28	0.32	**bcc Fe**
		0.350		0.52	0.34	0.32	Fe1
		0.348		0.84	0.38	0.35	Fe2
		0.306		1.26	0.12	0.01	Fe3

During acoustic cavitation, gas bubbles form, pulsate, and collapse in a treated liquid. The collapse of gas bubbles is accompanied by a concentrated release of energy; this results in several processes, including the emission of light, surface erosion, and the dispersion of solids [10]. High local temperatures and pressures, in combination with extremely fast cooling, provide unique opportunities for chemical reactions. In an ultrasonic wave field, water molecules decompose into free radicals. The subsequent reactions result in the formation of molecular hydrogen (H_2); hydrogen peroxide (H_2O_2); free radicals $\cdot H$, $\cdot OH$, $\cdot OH_2$, and $\cdot O_2H$; and solvated electrons. Hydrogen peroxide and radicals $\cdot OH_2$ and $\cdot O_2H$ are oxidants. Atomic hydrogen and solvated electrons are reducing agents. Ultrasonic treatment allowed us to obtain nanostructured metals, alloys, carbides, sulfides, stable colloids, and biomaterials [11].

In all our experiments with detected metal reduction, the suspensions contained an organic component.

CONCLUSIONS

The advantage of our technique is the proven reduction of oxidized iron forms to the metal state under the action of cavitation treatment.

ACKNOWLEDGMENTS

This work was supported by the RF Ministry of Education and Science's special program for Siberian Federal University; and by the Russian Foundation for Basic Research, project nos. 16-03-00969 and 15-42-04171 r_sibir'_a.

REFERENCES

1. Stolyar, S.V., Bayukov, O.A., Gurevich, Y.L., Denisova, E.A., Iskhakov, R.S., Ladygina, V.P., Puzyr', A.P., Pustoshilov, P.P., and Bitekhtina, M.A., *Inorg. Mater.*, 2006, vol. 42, no. 7, p. 763.

2. Stolyar, S.V., Bayukov, O.A., Gurevich, Y.L., Ladygina, V.P., Iskhakov, R.S., and Pustoshilov, P.P., *Inorg. Mater.*, 2007, vol. 43, no. 6, p. 638.

3. Dobretsov, K., Stolyar, S., and Lopatin, A., *Acta Otorhinolaryngol. Ital.*, 2015, vol. 35, no. 2, p. 97.

4. Ladygina, V.P., Purtov, K.V., Stolyar, S.V., Iskhakov, R.S., Bayukov, O.A., Gurevich, Yu.L., Dobretsov, K.G., and Ishchenko, L.A., RF Patent 2457074, 2012.

5. Inzhevatkin, E.V., Morozov, E.V., Khilazheva, E.D., Ladygina, V.P., Stolyar, S.V., and Falaleev, O.V., *Bull. Exp. Biol. Med.*, 2015, vol. 158, no. 6, p. 807.

6. Anghel, L., Balasoiu, M., Ishchenko, L.A., Stolyar, S.V., Kurkin, T.S., Rogachev, A.V., Kuklin, A.I., Kovalev, Y.S., Raikher, Y.L., Iskhakov, R.S., and Duca, G., *J. Phys.: Conf. Ser.*, 2012, vol. 351, p. 12005.

7. Michel, F.M., Ehm, L., Antao, S.M., Lee, P.L., Chupas, P.J., Liu, G., Strongin, D.R., Schoonen, M.A.A., Phillips, B.L., and Parise, J.B., *Science*, 2007, vol. 316, no. 5832, p. 1726.

8. Stolyar, S.V., Bayukov, O.A., Gurevich, Y.L., Iskhakov, R.S., and Ladygina, V.P., *Bull. Russ. Acad. Sci.: Phys.*, 2007, vol. 71, no. 9, p. 1286.

9. Amulyavichus, A.P. and Suzdalev, I.P., *J. Exp. Theor. Phys.*, 1973, vol. 37, no. 5, p. 859.

10. Margulis, M.A., *Osnovy zvukokhimii* (Foundations of Sonochemistry), Moscow: Vysshaya Shkola, 1984.

11. Doktycz, S.J. and Suslick, K.S., *Science*, 1990, vol. 247, no. 4946, p. 1067.

Translated by E. Bondareva